Journal of Hazardous Materials 340 (2017) 104–112

Contents lists available at ScienceDirect

Journal of Hazardous Materials

journal homepage: www.elsevier.com/locate/jhazmat

Simultaneous algae-polluted water treatment and electricity generation using a biocathode-coupled electrocoagulation cell (bio-ECC)

Yue Dong [a], Youpeng Qu [b,*], Chao Li [a], Xiaoyu Han [a], John J. Ambuchi [a], Junfeng Liu [a], Yanling Yu [a], Yujie Feng [a,*]

[a] State Key Laboratory of Urban Water Resource and Environment, Harbin Institute of Technology, No. 73 Huanghe Road, Nangang District, Harbin 150090, China
[b] School of Life Science and Technology, Harbin Institute of Technology, No. 2 Yikuang Street, Nangang District, Harbin 150080, China

HIGHLIGHTS

- A novel biocathode-coupled electrocoagulation cell (bio-ECC) was developed.
- Algae cell was removed by either settlement or electro-oxidation.
- A positive energy balance was still achieved at the cost of aeration in cathode.
- High efficiency in removal of NH_4^+-N by nitrifying biocathode.

GRAPHICAL ABSTRACT

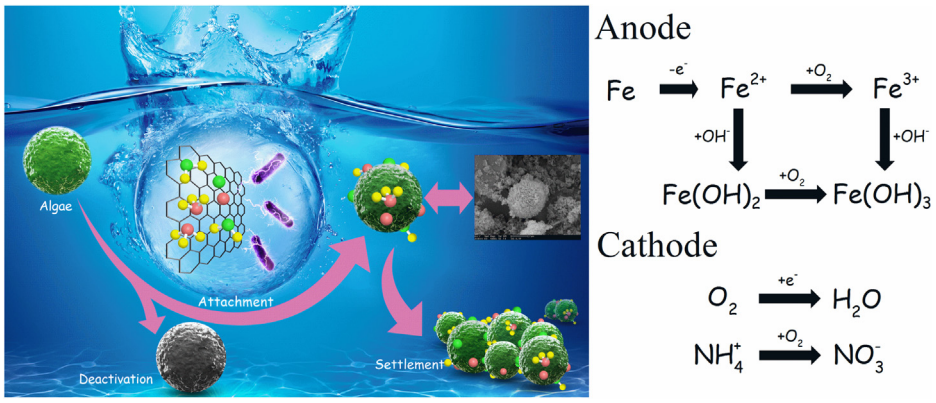

ARTICLE INFO

Article history:
Received 26 April 2017
Received in revised form 21 June 2017
Accepted 21 June 2017
Available online 23 June 2017

Keywords:
Biocathode-coupled electrocoagulation cell
Algae removal
Electricity generation
NH_4^+-N removal
Microbial community structure

ABSTRACT

How to utilize electrocoagulation (EC) technology for algae-polluted water treatment in an energy-efficient manner remains a critical challenge for its widespread application. Herein, a novel biocathode-coupled electrocoagulation cell (bio-ECC) with sacrificial iron anode and nitrifying biocathode was developed. Under different solution conductivities (2.33 ± 0.25 mS cm^{-1} and 4.94 ± 0.55 mS cm^{-1}), the bio-ECC achieved almost complete removal of algae cells. The maximum power densities of 8.41 and 11.33 W m^{-3} at corresponding current densities of 48.03 A m^{-3} and 66.26 A m^{-3} were obtained, with the positive energy balance of 4.52 and 7.44 W m^{-3}. In addition, the bio-ECC exhibited excellent NH_4^+-N removal performance with the nitrogen removal rates of 7.28 mg L^{-1} h^{-1} and 6.77 mg L^{-1} h^{-1} in cathode chamber, indicating the superiority of bio-ECC in NH_4^+-N removal. Pyrosequencing revealed that nitrifiers including *Nitrospira*, *Nitrobacter*, *Nitrosococcus*, and *Nitrosomonas* were enriched in biocathode. The removal mechanisms of algae in anode chamber were also explored by AFM and SEM-EDX tests. These results provide a proof-of-concept study of transferring energy-intensive EC process into an energy-neutral process with high-efficiency algae removal and electricity recovery.

* Corresponding authors.
E-mail addresses: qyp1000@163.com (Y. Qu), yujief@hit.edu.cn (Y. Feng).

http://dx.doi.org/10.1016/j.jhazmat.2017.06.055
0304-3894/

1. Introduction

Algal bloom is one of the major causes for aquatic environmental problems, exacerbating shortage of fresh water in today's society [1]. The outbreak of algae bloom can lead to deterioration of water quality by generating odour and taste, as well as organic matter contents [2]. Besides, it also poses difficulties in the process of drinking water treatment, as some of the extracellular algal product could add turbidity by interacting with flocculation and coagulation in raw water [3,4]. It is also believed that toxin release attributed to high algae population is a serious threat to human and animal health [5]. For example, a typical toxin-producing species belonging to *Microcystis* has made the World Health Organization (WHO) set the concentration limit for its associated toxin to 1 μg/L [6,7]. Thus, it is essential to enhance algae removal from algae-polluted water.

Commonly used technologies for algae removal are conventional processes, such as pre-oxidation by ozone or chlorine dioxide, combined membrane process, and coagulation process [8–10]. These technologies have been proved to be efficient in removing algae, but suffer from drawbacks of huge energy consumption and costly input, as well as poor environmental affinity. For example, ultrafiltration (UF) could only obtain stable removal of algae with increasing energy demand for maintaining a constant permeate flux because of permeability decline [11]. Some of the oxidizers or discharged chemical precipitates during pre-oxidation, such as permanganate or polyacrylamide [12], have great potential of polluting the ecosystem. Recently, several studies suggest that electrocoagulation (EC) technology may offer another preponderant option for algae removal [13]. A typical EC process involves three stages: in-situ coagulant generation (metal ions release), coagulation reaction, and solid-liquid separation [14]. The process offers many advantages: (1) Highly efficient and cost-effective sacrificial anode compared with traditional coagulant, such as aluminum or iron [15]; (2) The treatment process is easy to control because the electrochemical parameters can function as useful indicators of treatment level [16]; (3) Little adjustment in terms of pH, buffer type and concentration is needed for the reaction system [17]; (4) Absence of additional chemicals and pre-treatment is also a typical feature of EC process [18].

While EC process has been proven capable for algae removal, several barriers still remain unresolved to achieve further technological development. Firstly, high electrical energy demands make EC process unsustainable [19,20]. A lab-scale level of energy consumption of 0.20–2.28 kWh m^{-3} during algae removal was recorded [21]. Furthermore, energy loss could be exaggerated in a scaled system as a result of loss in circuit. Therefore, methods for energy-efficient operation are desirable. Secondly, high-concentration NH_4^+-N is a major incentive for algae bloom [22]. However, coagulant produced by aluminum or iron anode is less efficient for NH_4^+-N removal. The use of high applied voltage to EC system for direct electrochemical degradation of NH_4^+-N in electrode surface negates some of the technological advantages of using EC for real-world application [23]. Besides, effluent turning reddish-brown color remains as another challenge in use of iron anode which would cause sensory displeasure [24,25]. The color change is due to excessive coagulant production. This phenomenon is related to violent electrode reaction due to overqualified intensity of applied voltage, especially while treating heavily-polluted wastewaters [26]. It is also believed that an accelerated electrode passivation reaction under exaggerated applied voltage would occur, subsequently limiting the generation of coagulant and reducing service life of metal anode [24]. Therefore, obtaining an intensity-moderate reaction in anode is critical for sustainable operation of EC system.

During EC process, oxygen reduction reaction in the cathode is crucial in achieving high algae removal efficiency. Biocathode performs well microbial-catalyzed oxygen-reducing reaction in microbial fuel cell, which takes advantages in lower costs, longer service life and long-term performance sustainability for wastewater treatment [27,28]. Besides, efficient nitrification process for NH_4^+-N removal is also a typical feature of biocathode [29]. In a biocathode MFC, electrotrophic microorganisms accumulate on the cathode surface to uptake the electrons from anode for completion of whole electrochemical reaction. As previously reported, the activity of nitrification presented a synergetic relation with oxygen reduction [30]. Compared with noble metal catalysts such as Pt, microbial-catalyzed biocathode endows cathodic half-cell reaction with unique properties of mildness and controllability, which enables it to function as an ideal cathode system.

In this study, a novel biocathode-coupled electrocoagulation cell (bio-ECC) with sacrificial iron anode and nitrifying biocathode was constructed for algae-polluted water treatment. This system utilized the biocathode-catalyzed electricity generation process for simultaneous algae removal in anode and NH_4^+-N removal in cathode. The system performance in terms of algae removal, power generation under different electrolyte concentrations was investigated. Field-emission scanning electron microscope (SEM) coupled with energy-dispersive X-ray (EDX) analysis and atomic force microscopy (AFM) were employed to investigate the algae removal mechanisms in anode. Microbial similarity of the two biocathodes under different solution conductivities was also analyzed to determine if solution conductivity had an impact on community ecology.

2. Experiment section

2.1. Reactor configuration

The bio-ECC was comprised of two polymethylmethacrylate compartments, with the same cross-sectional dimension (5 cm long, 10 cm high). The thickness for anode chamber was 2 cm, while 4 cm for cathode chamber. The anode chamber and cathode chamber were separated by anion exchange membrane (AEM) to prevent the move of algae cells and positively-charged coagulant such as Fe^{2+} or Fe^{3+} between the two chambers. A piece of iron mesh (4 × 10 cm, mesh number of 30, wire diameter 0.3 mm) was used as anode, while the biocathode was carbon graphite fiber brush (4 cm diameter by 10 cm length). The total volume and working volume of the anode chamber were 100 mL and 80 mL, and corresponding values for cathode chamber were 200 mL and 160 mL. An air diffuser (4 cm outside diameter, Xiangsu Corporation, China) was located at the bottom of cathode chamber to inject air. The two chambers were clamped together by stainless steel fasteners and silica gel plates were inserted between membranes and chambers to prevent water leakage (Fig. 1).

2.2. Preparation of algal suspension and biocathode

Microcystis aeruginosa as one of the dominant cyanobacteria, responsible for occurrence of algal bloom in most parts of China, was used as the target algae in this study. It was obtained from Wuhan Institute of Hydrology of Chinese Academy of Sciences, and was cultivated in BG-11 medium as previously described [31]. The testing algal suspension was prepared by diluting the culture solution using deionized water to proper concentration with cell density of 1.4×10^{10}–1.6×10^{10} cell L^{-1}. All the testing algae were at the log growth phase.

The nitrifying biocathode was well-cultured in a two-chamber reactor with cation exchange membrane (CEM) as separator before

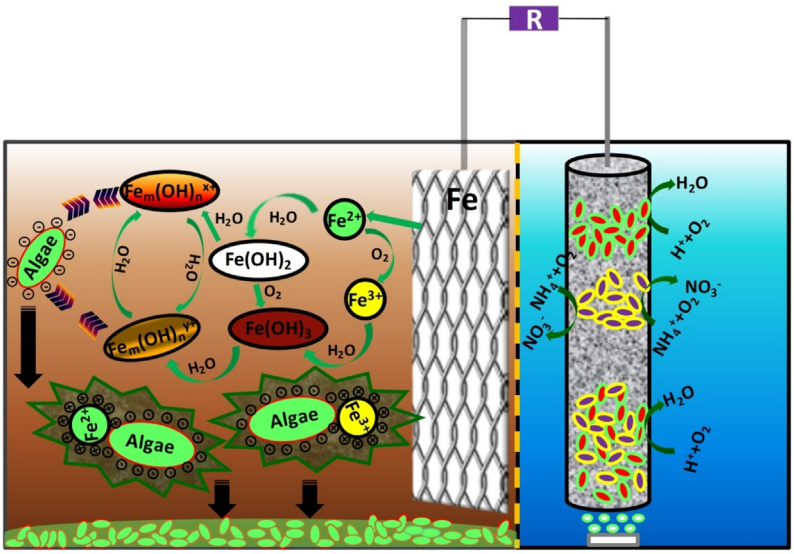

Fig. 1. Schematic diagrams of bio-ECC and the reactions in the anode and cathode.

installing into bio-ECC (detailed information in the SI). The cathode chamber of that two-chamber reactor was inoculated with domestic wastewater (50%, v/v), and the medium contained $NaHCO_3$ (1.0 g L^{-1}) and NH_4Cl (0.3 g L^{-1}) during the startup period. A phosphate buffered solution (KCl 0.13 g L^{-1}, $NaH_2PO_4{\cdot}2H_2O$, 3.32 g L^{-1}, $Na_2HPO_4{\cdot}12H_2O$, 10.32 g L^{-1}), tracer minerals and vitamins were added in the medium solution. The culture condition was the same as previously reported [32].

2.3. Bio-ECC operation

The solution used to simulate ammonia-rich algae-polluted water was prepared by adding the same substrate (NH_4Cl 0.3 g L^{-1} and Na_2CO_3 1 g L^{-1}), but set at different conductivities to investigate the performance of algae removal (NaCl 0 g L^{-1}, conductivity of 2.33 ± 0.25 mS cm^{-1}; NaCl 1 g L^{-1}, conductivity of 4.94 ± 0.55 mS cm^{-1}), with the characteristics shown in Table. 1. The synthetic algae-polluted water was first injected into anode chamber, with a detention time of 3 h. The supernatant of anolyte was then injected into cathode chamber, with a detention time of 6 h. The external resistance was kept at 50 Ω and 30 Ω in the absence and presence of NaCl, respectively. Fine air bubbles were supplied for aeration through air diffuser at the bottom of cathode chamber, at a rate of 15 mL min^{-1} (dissolved oxygen concentration at 2–3 mg L^{-1}). The anolyte was stirred with a magnetic stirrer to ensure the rapid diffusion of coagulant.

2.4. Measurement and analysis

About 3 mL anolyte was taken out every 0.5 h for algae removal, NH_4^+-N removal, and zeta potential analysis. Also, about 1 mL catholyte was taken out every 1 h for analysis of NH_4^+-N removal. The algae removal efficiency was calculated based on the algae counting with a microscope (BX51 Olympus, Japan) as previously reported [33]. The NH_4^+-N concentration was measured using a colorimeter according to the instructions of manufacturer (Hach Company, Loveland, CO). The zeta potential of anolyte was determined using a zeta potential analyzer (Nano-2, Malvern, UK).

The voltages of bio-ECC were recorded every 60 s by a data acquisition system (PISO-813, ICP DAS Co., Ltd.). The polarization curve was obtained by recording the current response to a linear potential decrease using the electrochemical workstation (Autolab PGSTAT128N, Metrohm Co., Swiss) at a scanning rate of 0.1 mV/s from open circuit to zero mV. The biocathode was set as working electrode, Fe anode as counter electrode and an Ag/AgCl electrode (+0.197 V vs. standard hydrogen electrode; SHE) as reference electrode. Power density was calculated by normalizing the power by total anode chamber volume.

The settled algal flocs at the bottom of anode chamber were observed by a field-emission scanning electron microscope (SEM, FEI Quanta 200F) coupled with energy-dispersive X-ray (EDX) analysis. Atomic force microscopy (AFM) (Bioscope Veeco, USA) was employed to further confirm the mechanisms for algae removal. Algal flocs were firstly rinsed in phosphate buffer (pH 7.0) to remove loosely attached impurities, then fixed on a glass slide. Imaging was performed after air drying in tapping mode using a probe.

2.5. Microbial community analysis

The bacterial communities of the biocathodes under different solution conductivities were analyzed by pyrosequencing at the end of the experiment. Total DNA was extracted from the samples using a MiniBEST Bacterial Genomic DNA Extraction Kit (TaKaRa Biotechnology, Japan) according to the manufacturer's instructions and assessed by electrophoresis in 1% agarose gels. The bacterial 16S rDNA PCR was performed using 338F and 806R Primers targeting the variable region V1–V3. Pyrosequencing of amplicons was performed by Sangon Biotech Company using MiSeq instrument. The similarity and difference between the two communities were depicted by Venn diagram with shared and unique OTUs [34].

3. Results and discussion

3.1. Electricity generation performance

The electricity generation performance by the bio-ECC was closely associated with the solution conductivity. The maximum power densities of the bio-ECC in the absence of NaCl was 8.41 W m^{-3} at a current density of 48.03 A m^{-3} (solution conductivity of 2.33 ± 0.25 mS cm^{-1}). With the increase in solution conductivity to 4.94 ± 0.55 mS cm^{-1} in the presence of 1 g L^{-1} NaCl, the maximum power density increased sharply by 35% to 11.33 W m^{-3} (current density of 66.26 A m^{-3}). The power densities produced by bio-ECC were comparable to these previously reported using biocathode MFCs (from 4.35 to 7.6 W m^{-3}) [35–37], but there

Table 1
Operation parameters of the bio-ECC.

Run	Influent concentration (g/L)			V_A (mL)	V_C (mL)	Aeration rate (mL min^{-1})	HRT_A (h)	HRT_C (h)	R_e (Ω)
	NH_4Cl	$NaHCO_3$	NaCl						
1	0.3	1	0	80	160	15	3	6	50
2	0.3	1	1						30

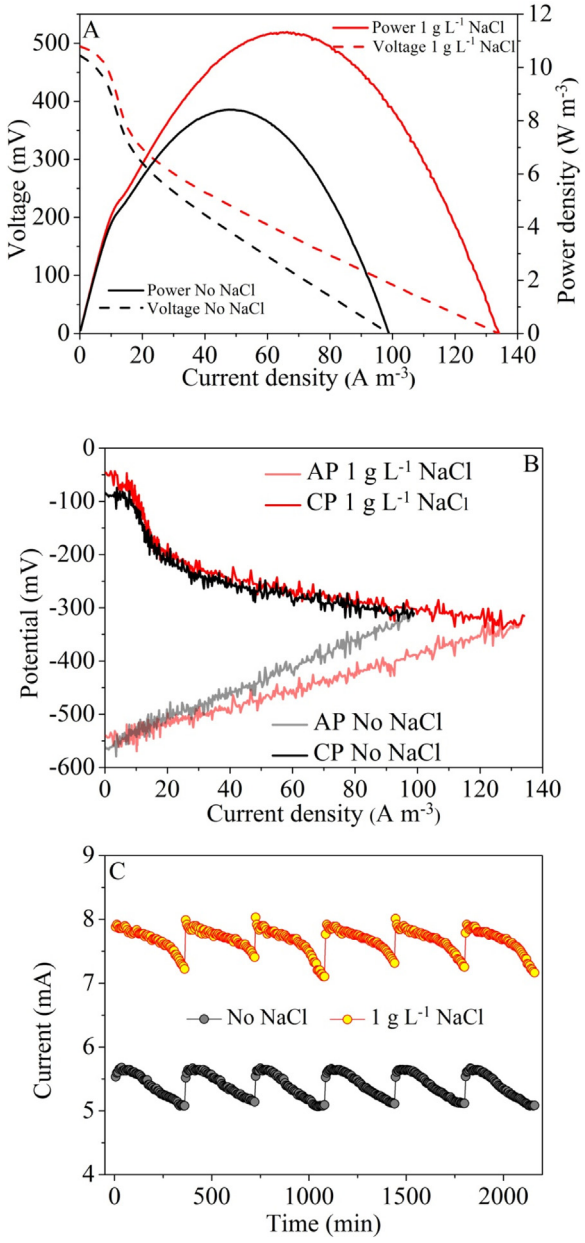

Fig. 2. (A) Power generation, (B) polarization curves, and (C) current generation of bio-ECC at different NaCl concentrations.

were many differences in these studies that precluded an accurate comparison of those values. The open circuit voltage (OCV) of bio-ECC with 1 g L^{-1} NaCl was 0.495 V, in comparison to 0.478 V when no NaCl was supplied to the solution (Fig. 2A). Polarization curves showed that the differences in power generation under different conditions were mainly caused by anode potential, while the cathode potential showed a slight difference with the variation of solution conductivity (Fig. 2B). The effect of conductivity on anode potential was more obvious at current densities higher than 15 A m^{-3}.

The bio-ECC with 1 g L^{-1} NaCl obtained a total internal resistance of 30 Ω. However, the total internal resistance when no NaCl was supplied was 66.7% higher than that with 1 g L^{-1} NaCl (50 Ω). At the external resistance of 30 Ω and 50 Ω, the average voltage output reached 0.23 ± 0.03 V and 0.26 ± 0.02 V under the two conditions (Fig. 2C). This result demonstrated that the increase in solution conductivity could lower ohmic resistance and improve ion fluxes between the electrodes. It was worth noting that algal bloom, as well as marine algal bloom, always occurred in company with highly-concentrated charged particles in polluted waters including ions and negatively-charged algae cells with a typical conductivity ranging from several to tens of millisiemens per cm. Therefore, such bio-ECC would exhibit enhanced electricity generation performance when treating algae-polluted water with high conductivity.

Noteworthily, aeration negated some of the energy-saving benefits in this bio-ECC system. The aeration power was calculated as 3.89 W m^{-3}, which was 46.3% of the power output of bio-ECC without NaCl input while only 34.3% when 1 g L^{-1} NaCl was supplied. Net power outputs of 4.52 and 7.44 W m^{-3} were obtained respectively. These results suggested that the bio-ECC was capable of turning the algae removal process into an energy-neutral operation, in spite of aeration in the biocathode.

3.2. Algae removal

The algae removal rate showed similar tendency as electricity generation performance. The bio-ECC with higher power output also possessed faster algae removal rate. More than 80% of the algae was removed at treatment time of 1 h (80.5 ± 3.2%) at the solution conductivity of 4.94 ± 0.55 mS cm^{-1}. With the decrease of solution conductivity to 2.33 ± 0.25 mS cm^{-1}, the bio-ECC merely obtained algae removal efficiency of 55.4 ± 4.1% with the same treatment time. The solution conductivity had little impact on algae removal in the final 1 h of treatment compared to its effect in the initial 1 h of treatment, with effluent achieving almost complete algae removal after 3 h treatment (Fig. 3A). A layer of algal flocs at the bottom of the reactor was observed with its color changing gradually from yellowish-green to reddish-brown, while the supernatant remained transparent. The flocs might be composed of Fe-bearing species and algae cells. The transparent supernatant indicated the appropriate production of coagulant by iron electrode, ensuring the sustainable operation of bio-ECC system.

Zeta potential is an indicator of effective surface charge which determines the dispersion stability of a particle [38]. The treatment process resulted in the increase of zeta potential of anolyte from −35.3 ± 1.56 mV to −9.76 ± 0.72 mV at the solution conductivity of 2.33 ± 0.25 mS cm^{-1}. This trend of reduction in zeta potential from a large value to small value indicated that the flocs changed from steady-state particles to destabilized particles. The corresponding variation from −27.35 ± 0.64 mV to −4.35 ± 0.87 mV was also observed at the solution conductivity of 4.94 ± 0.55 mS cm^{-1} (Fig. 3B). The final zeta potential which was more closer to zero demonstrated that the supply of NaCl could increase the destabi-

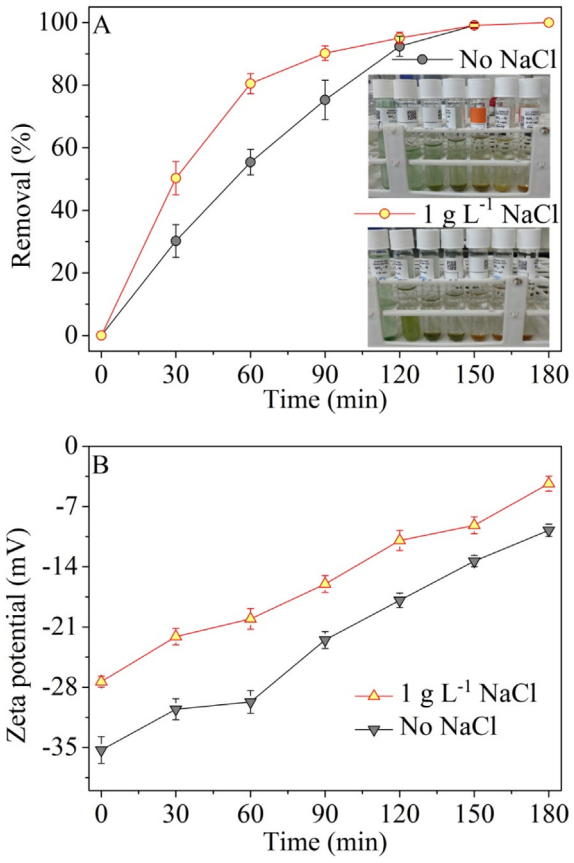

Fig. 3. (A) Algae cell removal, (B) variation of zeta potential during the operation at different NaCl concentrations.

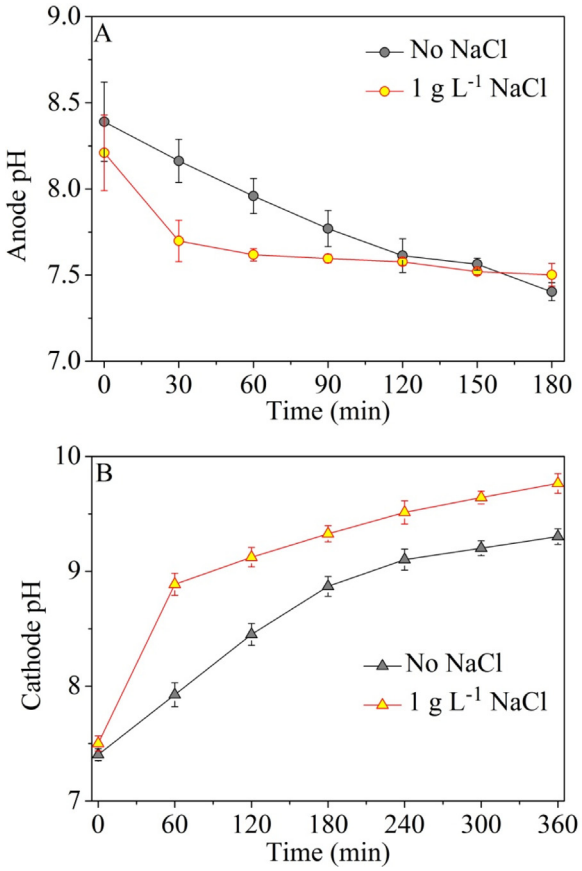

Fig. 4. Variation of pH in anode (A) and cathode (B) chambers during the operation time at different NaCl concentrations.

lization capacity of the flocs and facilitate solid-liquid separation of algae.

Solution pH is one of the key parameters influencing the EC process in anode. In this study, the anolyte pH dropped gradually from 8.39 ± 0.23 to 7.40 ± 0.05 at the solution conductivity of 2.33 ± 0.25 mS cm^{-1}. However, with the addition of NaCl, it exhibited a rapid decrease in the first 0.5 h, and then remained relatively constant (7.50–7.69) (Fig. 4A). This decrease of anolyte pH was due to the consumption of OH^- by Fe^{2+} produced by iron anode forming precipitation of iron hydroxide. At higher solution conductivity, faster anode reaction resulted in release of more Fe^{2+} into the solution, accounting for the rapid decrease of anolyte pH in the initial 0.5 h. The move of OH^- from cathode chamber to anode chamber derived from internal electric field led to relatively constant anolyte pH in the following treatment process. These pH variations were different from that in previous EC process, where solution pH increased as the increase of electrolysis time [39]. This was attributed to the independent processes of flocculant generation in anode and alkalinity production in cathode of bio-ECC, while traditional EC process occurred in a single chamber with in-situ alkalinity production in cathode.

3.3. The algae removal mechanisms

Three mechanisms are possibly responsible for the algae removal in this study. Firstly, due to the potential difference of iron anode and biocathode, Fe^{2+} was generated and released into solution in anode chamber, some of which were oxidized to Fe^{3+} because of dissolved oxygen in anolyte. Electrostatic attractive force between positively-charged iron ions and negatively-charged algae cells was enhanced. Thus, those algae cells lost electrostatic repulsive force between each other, followed by decline in system dispersion stability, in favor of algae sedimentation. Secondly, some of iron hydroxides, such as $Fe(OH)_2$ and $Fe(OH)_3$, might help to improve the efficiency of algae removal through the sweeping and enmeshment effect. Thirdly, it has been reported that deactivation of algae cells could be triggered as a result of oxidation of coenzyme A (CoA), as it plays an important role in cell respiration [40]. In this study, the negatively-charged algae cells were absorbed on the surface of iron anode under the electric field force. Electro-oxidation of these algae cells by direct electron exchange between cells and electrode might also account for a portion of algae removal [41].

For better understanding of the removal mechanism of algae, the surface morphology of algae cells were analyzed by AFM (Fig. 5). The fresh algae cells exhibited smooth surface and distinct cell contour. However, the algae cell surface appeared to be ravined after EC treatment, with cell boundary becoming blurred. A number of small floccules were adsorbed on the cell surface because of charge neutralization between the positively-charged floccules and the negatively-charged algae cells. The addition of NaCl resulted in the burst of some algae cells, in the company of outflow of cellular contents, which might be due to direct electro-oxidation. This AFM result confirmed that the algae cells were removed by direct interaction of negatively-charged algae cells with either positively-charged iron coagulant or electrode itself.

To further explore the removal mechanism, SEM-EDX was applied to analyze the composition of flocs (Fig. 6). It could be observed that algae cells were covered by floccules, and the supply of NaCl in the influent could result in more floccules in the flocs. Two sites on the algae flocs were investigated through EDX analy-

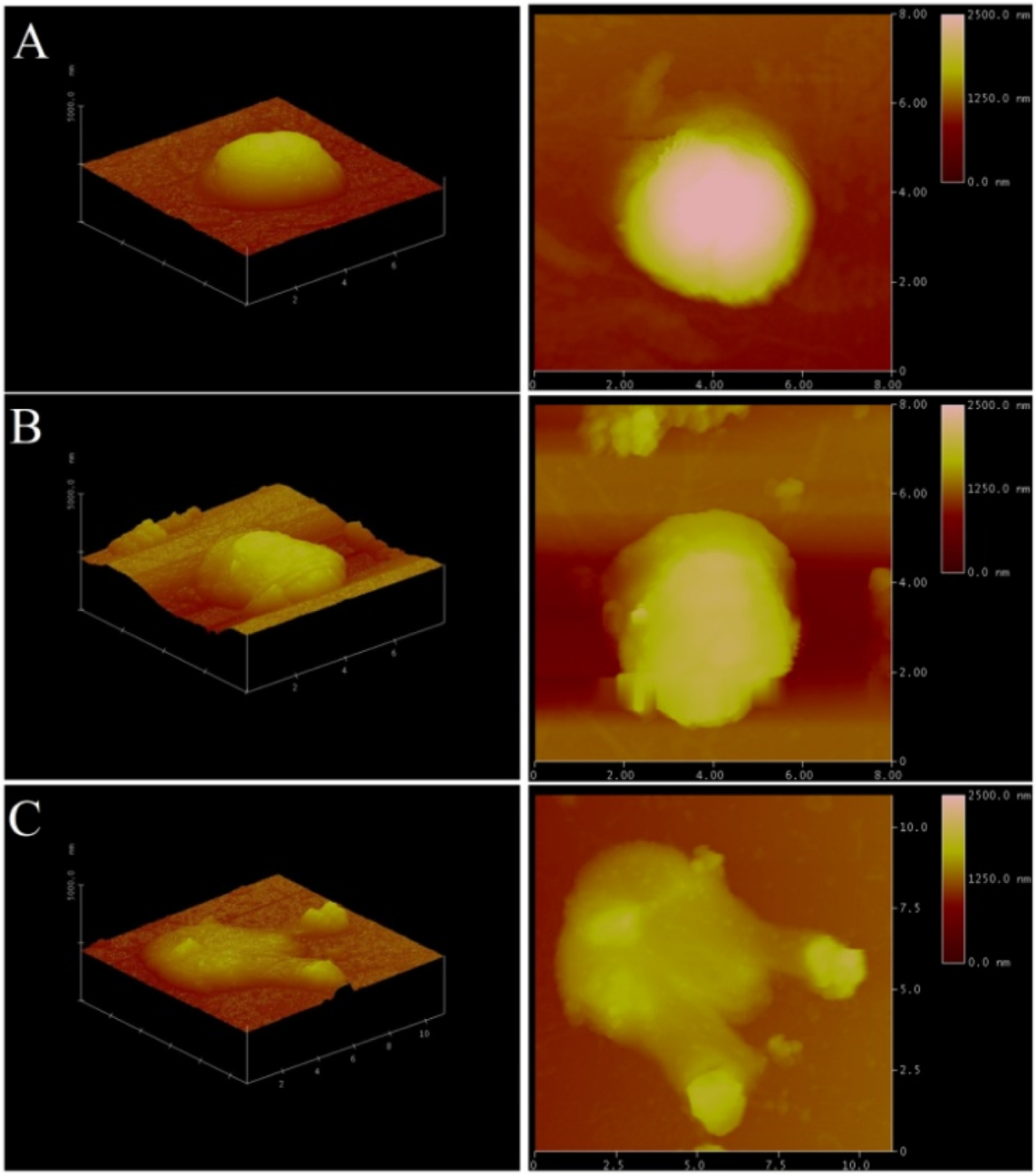

Fig. 5. AFM topographic image of algae cell, scan rate: 0.5 Hz. (A) Algae in fresh culture before treatment, (B) after bio-ECC treatment at NaCl concentration 0 g/L, (C) after bio-ECC treatment at NaCl concentration 1 g/L.

sis under the two solution conductivities. One site was on the algae cell (spectrum 1 and 3), while the other site was on the agglutinant (spectrum 2 and 4). The algae cell was mainly consisted of carbon, nitrogen and oxygen contents. The contents of carbon, nitrogen and oxygen in the agglutinant were similar with that in algae cell. This was probably caused by the release of cell fragments into agglutinant. Fe element (31.27% in spectrum 1 and 31.83% in spectrum 3) was detected on the algae cell as expected, and its mass ratio was lower than that in the agglutinant (39.36% in spectrum 1 and 45.41% in spectrum 3). This mass ratio result of Fe element further demonstrated that algae cells were removed after the attachment of iron coagulant to algae cells. An increase of 6.05% in Fe content of the agglutinant was observed when NaCl was added, indicating a faster anode reaction kinetics compared to that without the additional NaCl input.

3.4. The performance of biocathode

The coagulant produced by Fe anode presented to be less efficient for NH_4^+-N removal as influent and effluent NH_4^+-N concentrations were almost identical. In biocathode, NH_4^+-N removal ($55.7 \pm 2.1\%$) without NaCl in the influent was slightly higher compared to the addition of NaCl ($51.7 \pm 2.3\%$), with the nitrogen removal rates of 7.28 mg L^{-1} h^{-1} and 6.77 mg L^{-1} h^{-1} respectively (Fig. 7A). The catalytic activity of biocathode in terms of oxygen reduction and nitrification was strongly related to solution pH. The pH of catholyte under both influent conductivities increased rapidly during the initial 2 h, and then increased slowly after that due to migration of OH^- to anode chamber. Besides, nitrification process producing acidity, to some extent, also slowed down the rise of pH. A little difference of final pH between the two influent conduc-

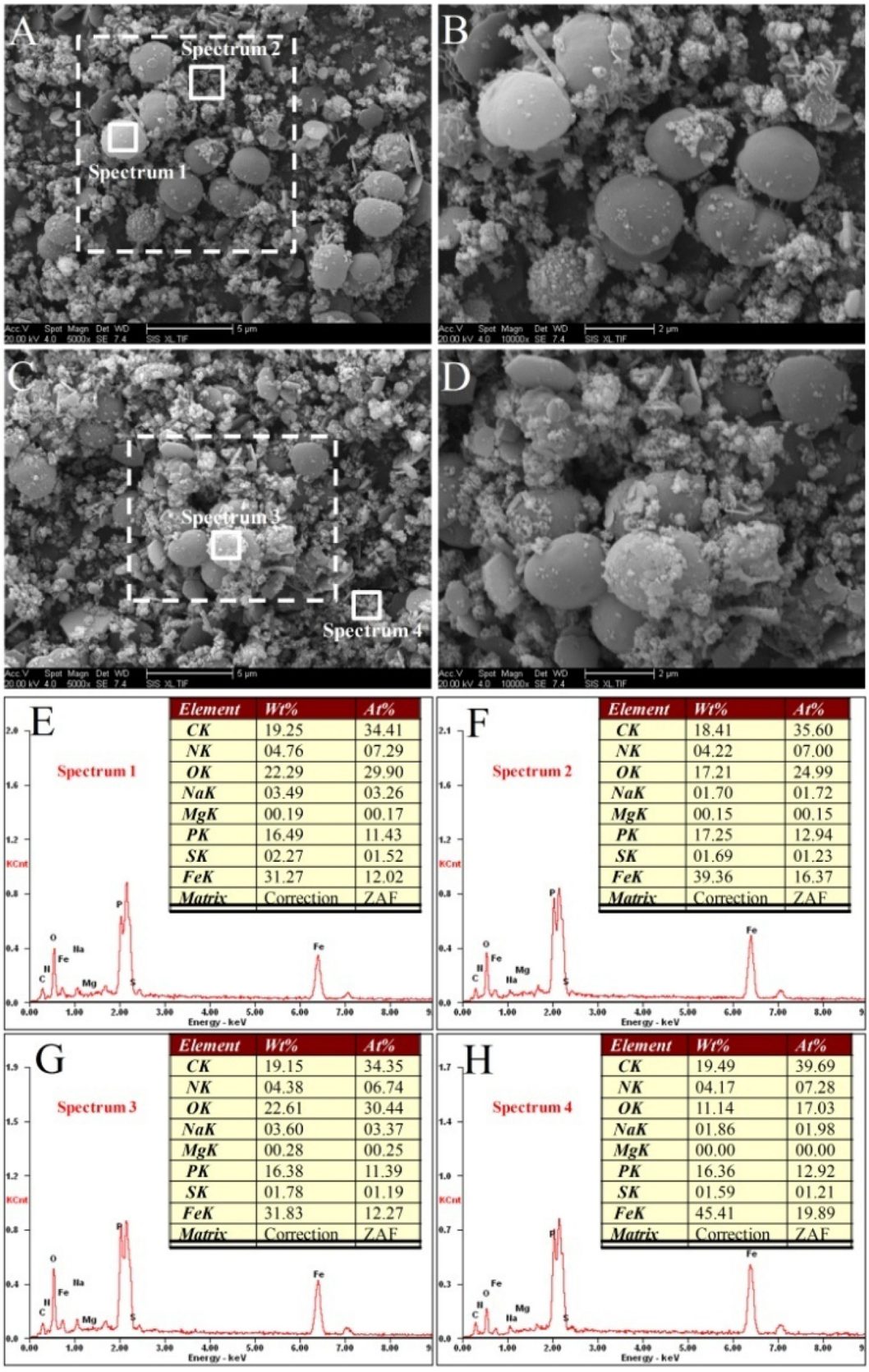

Fig. 6. SEM-EDX analysis of the algal flocs produced. SEM micrograph at different magnification: (A)–(B) at NaCl concentration 0 g/L and (C)–(D) at NaCl concentration 1 g/L, (E)–(H) EDX analysis of elemental composition on the algae cells and on the agglutinant.

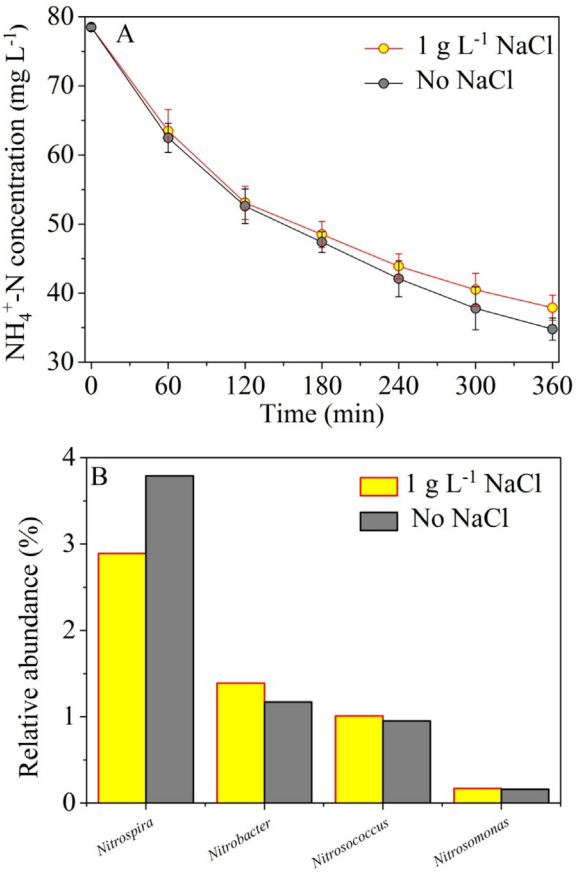

Fig. 7. (A) Degradation of NH_4^+-N in the cathode chamber, (B) relative abundance of nitrifiers retrieved from biocathodes at different NaCl concentrations.

tivities was observed (9.30 ± 0.07, without NaCl; 9.77 ± 0.09, with NaCl) (Fig. 4B). The relatively higher pH with addition of NaCl was attributed to better electricity generation performance that consumed more protons and released more hydroxyl anions into the solution.

The bacterial community structures of biocathodes under different influent conductivities were characterized by pyrosequencing. Up to 26044 qualified sequencing reads were yielded at low influent conductivity (C-1), which were clustered to 401 operational taxonomic units (OTUs) on the basis of more than 97% sequence similarity. About 23593 qualified sequencing reads (391 OTUs) were obtained when NaCl was supplied in the influent (C-2). The sum of observed OTUs with a relative abundance higher than 1% was 23, while 20 OTUs were in common between the two samples. Phylogenetic diversity of bacterial communities on two kinds of biocathodes based on phylum (Fig. S1A) and family (Fig. S1B) levels further demonstrated the high similarity between them. For example, the bacteria communities consisted of almost same structure with the dominance of *Proteobacteria* (a part of *Proteobacteria* families are generally called "exoelectrogens") at phylum level with a relative abundance of 53.12% in C-1 and 53.6% in C-2 [42]. These exoelectrogens played an important role in cathode reaction for oxygen reduction. Both the two samples were enriched with nitrifiers [43] including *Nitrospira*, *Nitrobacter*, *Nitrosococcus*, *Nitrosomonas* with a total abundance of 3.79%, 1.17%, 0.95% and 0.16% in C-1, with the corresponding values for C-2 being 2.89%, 1.39%, 1.01% and 0.17% (Fig. 7B), respectively. The enrichment of nitrifiers on biocathode ensured the high-efficiency removal of NH_4^+-N in the cathode chamber.

In the light of the above results, the variation of solution conductivity did not significantly change microbial community on biocathode. This high similarity between bacterial communities under different solution conductivities demonstrated that the biocathode had strong resistance to salinity fluctuation. This indicated a possibility of using bio-ECC for treatment of heavily-polluted wastewaters with high salinity or marine algal bloom. Besides, the biocathode could function well without inhibition from metal ions when coupled with metal anode as in other microbial electrochemical systems, evidenced by the abundant electrographic microorganisms.

Taken together, as an effective integration of EC process and microbial-catalyzed electricity generation process, bio-ECC represented a promising method for treatment of algae-polluted water. Three separate innovations were highlighted to promote its application. (1) Direct electricity generation and positive energy balance in algae removal process: although aeration in bioctahode shadowed the feature of electricity generation, positive energy balance could still be obtained, which overcame the limitation of huge energy input in traditional EC process. (2) Efficient NH_4^+-N removal: microbial-catalyzed nitrification process eliminated the need of direct electrochemical oxidization of NH_4^+-N, demonstrating excellent environmental affinity. (3) Offering effective means for process control. Spontaneous electricity generation made anode reaction produce proper amount of coagulant inherently amendable by adjusting external resistor, avoiding electrode passivation or high-chroma supernatant caused by excessive electrode reaction. Notwithstanding, there still remained several challenges to be overcome for possible application. For example, bio-ECC for real algae-polluted water treatment has not yet been examined. With further studies, better evaluation of bio-ECC in terms of technological possibility could be performed.

4. Conclusions

In summary, a novel bio-ECC based on sacrificial iron anode and nitrifying biocathode was designed and proved feasible to treat algae-polluted water. The system achieved almost complete algae removal at different influent conductivities. In addition, the bio-ECC also exhibited high NH_4^+-N removal efficiency (55.7 ± 2.1% and 51.7 ± 2.3%) with the nitrogen removal rates of 7.28 mg L^{-1} h^{-1} and 6.77 mg L^{-1} h^{-1}. Nitrifiers including *Nitrospira*, *Nitrobacter*, *Nitrosococcus*, *Nitrosomonas* were detected in biocathode, which ensured the efficient removal of NH_4^+-N. The direct electricity generations of bio-ECC were 8.41 and 11.33 W m^{-3}, resulting in net power outputs of 4.52 and 7.44 W m^{-3} when taking the aeration consumption into account. These results demonstrate that the nitrifying biocathode could be effectively coupled with EC process for algae-polluted water treatment.

Acknowledgements

This work was supported by the China Postdoctoral Science Foundation (2016M591534), The Heilongjiang Postdoctoral Fund (LBH-Z16088), the National Natural Science Fund for Distinguished Young Scholars (Grant No. 51125033) and National Natural Science Fund for Young Scholars (Grant No. 51209061). The author also acknowledgment the supports by the International Cooperating Project between China and European Union (Grant No. 2014DFE90110) and supports from the State Key Lab of Urban Water Resource and Environment (2015DX08).

Appendix A. Supplementary data

Supplementary data associated with this article can be found, in the online version, at http://dx.doi.org/10.1016/j.jhazmat.2017.06.055.

References

[1] L.M. Grattan, S. Holobaugh, J.G. Morris Jr., Harmful algal blooms and public health, Harmful Algae 57 (2016) 2–8.
[2] W.W. Driscoll, J.D. Hackett, R. Ferriere, Eco-evolutionary feedbacks between private and public goods: evidence from toxic algal blooms, Ecol. Lett. 19 (2016) 81–97.
[3] W. Huang, H. Chu, B. Dong, M. Hu, Y. Yu, A membrane combined process to cope with algae blooms in water, Desalination 355 (2015) 99–109.
[4] X. Tang, H. Zheng, B. Gao, C. Zhao, B. Liu, Interactions of specific extracellular organic matter and polyaluminum chloride and their roles in the algae-polluted water treatment, J. Hazard. Mater. 332 (2017) 1–9.
[5] B.W. Brooks, J.M. Lazorchak, M.D. Howard, M.V. Johnson, S.L. Morton, D.A. Perkins, E.D. Reavie, G.I. Scott, S.A. Smith, J.A. Steevens, Are harmful algal blooms becoming the greatest inland water quality threat to public health and aquatic ecosystems? Environ. Toxicol. Chem. 35 (2016) 6–13.
[6] E. Dittmann, C. Wiegand, Cyanobacterial toxins–occurrence, biosynthesis and impact on human affairs, Mol. Nutr. Food Res. 50 (2006) 7–17.
[7] WHO, Guidelines for Drinking Water Quality: Addendum to Volume 1-Recomendations, World Health Organisation, Geneva, 1998.
[8] J.J. Chen, H.H. Yeh, I.C. Tseng, Effect of ozone and permanganate on algae coagulation removal–pilot and bench scale tests, Chemosphere 74 (2009) 840–846.
[9] H. Liang, W. Gong, J. Chen, G. Li, Cleaning of fouled ultrafiltration (UF) membrane by algae during reservoir water treatment, Desalination 220 (2008) 267–272.
[10] Q. Zhang, B. Liu, Y. Liu, Effect of ozone on algal organic matters as precursors for disinfection by-products production, Environ. Technol. 35 (2014) 1753–1759.
[11] B. Kwon, N. Park, J. Cho, Effect of algae on fouling and efficiency of UF membranes, Desalination 179 (2005) 203–214.
[12] R. Henderson, S.A. Parsons, B. Jefferson, The impact of algal properties and pre-oxidation on solid-liquid separation of algae, Water Res. 42 (2008) 1827–1845.
[13] M.M. Emamjomeh, M. Sivakumar, Review of pollutants removed by electrocoagulation and electrocoagulation/flotation processes, J. Environ. Manag. 90 (2009) 1663–1679.
[14] C.Y. Hu, S.L. Lo, W.H. Kuan, Effects of co-existing anions on fluoride removal in electrocoagulation (EC) process using aluminum electrodes, Water Res. 37 (2003) 4513–4523.
[15] F. Ilhan, U. Kurt, O. Apaydin, M.T. Gonullu, Treatment of leachate by electrocoagulation using aluminum and iron electrodes, J. Hazard. Mater. 154 (2008) 381–389.
[16] S. Zaidi, T. Chaabane, V. Sivasankar, A. Darchen, R. Maachi, T.A.M. Msagati, M. Prabhakaran, Performance efficiency of electro-coagulation coupled electro-flotation process (EC-EF) versus adsorption process in doxycycline removal from aqueous solutions, Process. Saf. Environ. 102 (2016) 450–461.
[17] J. Ge, J. Qu, P. Lei, H. Liu, New bipolar electrocoagulation–electroflotation process for the treatment of laundry wastewater, Sep. Purif. Technol. 36 (2004) 33–39.
[18] M. Ben-Sasson, Y. Zidon, R. Calvo, A. Adin, Enhanced removal of natural organic matter by hybrid process of electrocoagulation and dead-end microfiltration, Chem. Eng. J. 232 (2013) 338–345.
[19] M. Ren, Y. Song, S. Xiao, P. Zeng, J. Peng, Treatment of berberine hydrochloride wastewater by using pulse electro-coagulation process with Fe electrode, Chem. Eng. J. 169 (2011) 84–90.
[20] I. Zongo, J.-P. Leclerc, H.A. Maïga, J. Wéthé, F. Lapicque, Removal of hexavalent chromium from industrial wastewater by electrocoagulation: a comprehensive comparison of aluminium and iron electrodes, Sep. Purif. Technol. 66 (2009) 159–166.
[21] S. Gao, J. Yang, J. Tian, F. Ma, G. Tu, M. Du, Electro-coagulation-flotation process for algae removal, J. Hazard. Mater. 177 (2010) 336–343.
[22] C. Yan, F. Che, L. Zeng, Z. Wang, M. Du, Q. Wei, Z. Wang, D. Wang, Z. Zhen, Spatial and seasonal changes of arsenic species in Lake Taihu in relation to eutrophication, Sci. Total. Environ. 563 (2016) 496–505.
[23] Y. Tian, W. He, X. Zhu, W. Yang, N. Ren, B.E. Logan, Energy efficient electrocoagulation using an air-breathing cathode to remove nutrients from wastewater, Chem. Eng. J. 292 (2016) 308–314.
[24] H. Cesar Lopes Geraldino, J. Izabelle Simionato, T. Karoliny Formicoli de Souza Freitas, J. Carla Garcia, N. Evelázio de Souza, Evaluation of the electrode wear and the residual concentration of iron in a system of electrocoagulation, Desalin. Water Treat. 57 (2015) 13377–13387.
[25] G. Chen, Electrochemical technologies in wastewater treatment, Sep. Purif. Technol. 38 (2004) 11–41.
[26] P.K. Holt, G.W. Barton, C.A. Mitchell, The future for electrocoagulation as a localised water treatment technology, Chemosphere 59 (2005) 355–367.
[27] G. Zhang, Q. Zhao, Y. Jiao, K. Wang, D.J. Lee, N. Ren, Biocathode microbial fuel cell for efficient electricity recovery from dairy manure, Biosens. Bioelectron. 31 (2012) 537–543.
[28] P.J. Cai, X. Xiao, Y.R. He, W.W. Li, G.L. Zang, G.P. Sheng, M.H. Lam, L. Yu, H.Q. Yu, Reactive oxygen species (ROS) generated by cyanobacteria act as an electron acceptor in the biocathode of a bio-electrochemical system, Biosens. Bioelectron. 39 (2013) 306–310.
[29] Y. Du, Y. Feng, Y. Dong, Y. Qu, J. Liu, X. Zhou, N. Ren, Coupling interaction of cathodic reduction and microbial metabolism in aerobic biocathode of microbial fuel cell, RSC Adv. 4 (2014) 34350.
[30] Y. Du, Y. Feng, Y. Qu, J. Liu, N. Ren, H. Liu, Electricity generation and pollutant degradation using a novel biocathode coupled photoelectrochemical cell, Environ. Sci. Technol. 48 (2014) 7634–7641.
[31] Y. Xu, J. Yang, M. Ou, Y. Wang, J. Jia, Study of Microcystis aeruginosa inhibition by electrochemical method, Biochem. Eng. J. 36 (2007) 215–220.
[32] D.R. Lovley, E.J. Phillips, Novel mode of microbial energy metabolism: organic carbon oxidation coupled to dissimilatory reduction of iron or manganese, Appl. Environ. Microbiol. 54 (1988) 1472–1480.
[33] J.D. Brookes, G.G. Ganf, M.D. Burch, Separation of forms of *Microcystis* from *Anabaena* in mixed populations by the application of pressure, Mar. Freshw. Res. 45 (1994) 863–868.
[34] L. Lu, D. Xing, N. Ren, Pyrosequencing reveals highly diverse microbial communities in microbial electrolysis cells involved in enhanced H2 production from waste activated sludge, Water Res. 46 (2012) 2425–2434.
[35] Y.K. Wang, G.P. Sheng, W.W. Li, Y.X. Huang, Y.Y. Yu, R.J. Zeng, H.Q. Yu, Development of a novel bioelectrochemical membrane reactor for wastewater treatment, Environ. Sci. Technol. 45 (2011) 9256–9261.
[36] Y.-K. Wang, G.-P. Sheng, B.-J. Shi, W.-W. Li, H.-Q. Yu, A novel electrochemical membrane bioreactor as a potential net energy producer for sustainable wastewater treatment, Sci. Rep. 3 (2013) 1864.
[37] Y.P. Wang, X.W. Liu, W.W. Li, F. Li, Y.K. Wang, G.P. Sheng, R.J. Zeng, H.Q. Yu, A microbial fuel cell–membrane bioreactor integrated system for cost-effective wastewater treatment, Appl. Energy 98 (2012) 230–235.
[38] D. Gregory, K. Carlson, Relationship of pH and floc formation kinetics to granular media filtration performance, Environ. Sci. Technol. 37 (2003) 1398–1403.
[39] F. Baierle, D.K. John, M.P. Souza, T.R. Bjerk, M.S.A. Moraes, M. Hoeltz, A.L.B. Rohlfes, M.E. Camargo, V.A. Corbellini, R.C.S. Schneider, Biomass from microalgae separation by electroflotation with iron and aluminum spiral electrodes, Chem. Eng. J. 267 (2015) 274–281.
[40] T. Matsunaga, S. Nakasono, T. Takamuku, J.G. Burgess, N. Nakamura, K. Sode, Disinfection of drinking water by using a novel electrochemical reactor employing carbon-cloth electrodes, Appl. Environ. Microb. 58 (1992) 686–689.
[41] L.-C. Chiang, J.E. Chang, T.C. Wen, Indirect oxidation effect in electrochemical oxidation treatment of landfill leachate, Water Res. 29 (1995) 671–678.
[42] D.R. Lovley, The microbe electric: conversion of organic matter to electricity, Curr. Opin. Biotechnol. 19 (2008) 564–571.
[43] R. Cui, W.J. Chung, D. Jahng, A rapid and simple respirometric biosensor with immobilized cells of Nitrosomonas europaea for detecting inhibitors of ammonia oxidation, Biosens. Bioelectron. 20 (2005) 1788–1795.